Published in final edited form as:

Nat Chem Biol. 2013 April ; 9(4): 257–263. doi:10.1038/nchembio.1183.

Photochemical activation of TRPA1 channels in neurons and animals

David Kokel[1,2,*], **Chung Yan J. Cheung**[1,2], **Robert Mills**[1], **Jaeda Coutinho-Budd**[3], **Liyi Huang**[5,6,7], **Vincent Setola**[9], **Jared Sprague**[10], **Shan Jin**[1,2], **Youngnam N. Jin**[1,2], **Xi-Ping Huang**[9], **Giancarlo Bruni**[1], **Clifford Woolf**[10], **Bryan L. Roth**[9], **Michael R Hamblin**[5,6,7,8], **Mark J. Zylka**[3,4], **David J. Milan**[1], and **Randall T. Peterson**[1,2,*]

[1]Cardiovascular Research Center and Division of Cardiology, Department of Medicine, Massachusetts General Hospital, Harvard Medical School, 149 13th Street, Charlestown, Massachusetts, 02129, USA

[2]Broad Institute, 7 Cambridge Center, Cambridge, Massachusetts 02142, USA

[3]UNC Neuroscience Center, University of North Carolina at Chapel Hill, CB #7545, Chapel Hill, NC 27599

[4]Department of Cell and Molecular Physiology, University of North Carolina at Chapel Hill, CB #7545, Chapel Hill, NC 27599

[5]Wellman Center for Photomedicine, Massachusetts General Hospital, Boston, MA 02114

[6]Department of Dermatology, Harvard Medical School, Boston, MA 02115

[7]Department of Infectious Diseases, First Affiliated College & Hospital, Guangxi Medical University, Nanning, China 530021

[8]Harvard-MIT Division of Health Sciences and Technology, Cambridge, MA 02139

[9]Department of Pharmacology and NIMH Psychoactive Drug Screening Program, University of North Carolina Chapel Hill Medical School, Chapel Hill, NC 27759

[10]Neurobiology Department, Children's Hospital Boston, Harvard Medical School, Boston, MA 02115

Abstract

Optogenetics is a powerful research tool because it enables high-resolution optical control of neuronal activity. However, current optogenetic approaches are limited to transgenic systems expressing microbial opsins and other exogenous photoreceptors. Here, we identify optovin, a small molecule that enables repeated photoactivation of motor behaviors in wild type animals.

*dkokel@cvrc.mgh.harvard.edu or peterson@cvrc.mgh.harvard.edu.

Competeing financial interests The authors declare no competing financial interests.

AUTHOR CONTRIBUTIONS DK designed and performed the research, analyzed the data and wrote the manuscript with RTP. CYJC, RM, JC-B, LH, VS, JS, SJ, YNJ and X-PH designed and performed the experiments and interpreted data. CW, BLR, MRH, MJZ and DJM analyzed and interpreted the data. All authors contributed to data interpretation and commented on the manuscript.

Surprisingly, optovin's behavioral effects are not visually mediated. Rather, photodetection is performed by sensory neurons expressing the cation channel TRPA1. TRPA1 is both necessary and sufficient for the optovin response. Optovin activates human TRPA1 via structure-dependent photochemical reactions with redox-sensitive cysteine residues. In animals with severed spinal cords, optovin treatment enables control of motor activity in the paralyzed extremities by localized illumination. These studies identify a light-based strategy for controlling endogenous TRPA1 receptors *in vivo*, with potential clinical and research applications in non-transgenic animals, including humans.

Introduction

One of the most influential recent innovations in neuroscience has been optogenetics, an approach for controlling neurons with exogenous microbial opsins or other ectopic photosensitive channels[1–11]. Optogenetic techniques in model organisms are yielding remarkable new insights in neuroscience and medicine. However, current approaches do not address the unmet need for controlling endogenous neuronal proteins and neuronal signaling in non-transgenic animals with light.

Photochemical tools for controling endogenous channels *in vivo* enable powerful approaches for neuroscience research and therapeutic intervention[12]. For example, photorelease of caged glutamate provides optical control of glutamate receptors in brain slices. Azobenzene-containing photoswitchable ligands also provide optical control glutamate receptors and potassium channels[9,10,12–19]. However, virtually all prior work in chemical optogenetics has been limited to cultured cells, tissue slices, and other *ex vivo* preparations because most existing techniques are not effective *in vivo*. Discovery of new compounds with higher potency and better *in vivo* properties would improve the photochemical ligand toolbox. Here, we used behavior-based chemical screening to identify optovin, a novel photochemical switch compound with potent bioactivity in intact living animals.

Receptors in the transient receptor potential (TRP) family are attractive channels for bringing under optical control[20]. TRP channels are involved in diverse sensory systems including vision, taste, temperature and touch. TRPA1 signaling contributes to illnesses including neuropathic pain and chronic inflammation[21–24]. Precise control of TRPA1 channels may have utility for understanding and treating these disorders. However, currently available TRPA1 ligands like mustard oil and cinnamaldehyde provide imprecise spatiotemporal control of TRPA1 signaling.

Here, we used a behavior-based chemical screening approach to identify optovin, a novel neuroactive small molecule. Optovin is a TRPA1 ligand that can be reversibly photoactivated by violet light. Optovin's behavioral effects depend on TRPA1 and shows activity on zebrafish, mouse neurons, and recombinant human protein. The photochemical reaction mechanism likely involves reversible covalent thioether bonding between TRPA1 and optovin. Optovin is the first known photochemical TRPA1 ligand. Optovin enables optical control of neurons that express this target in wild type animals.

Results

Behavior-based chemical screening identifies optovin

To identify small molecules for the optical control of endogenous channels, we screened for compounds that could drive light-dependent motor behaviors in wild-type zebrafish. Zebrafish embryos are uniquely well suited for phenotype based chemicals screens[25,26]. They are blind for the first 3 days of development and other than a one-time motor response to the first light exposure in dark-adapted animals (the photomotor response, PMR), zebrafish embryos are unresponsive to light[27,28] (Fig 1a, Supplementary Results, Supplementary Movie 1). We screened a library of 10,000 structurally diverse synthetic small molecules for compounds that render zebrafish embryos responsive to light. Behavioral responses were measured for each well in comparison to a set of 2,500 DMSO treated controls. This screen identified a single compound, optovin, which increased motor activity greater than 40 standard deviations above the control mean (Fig. 1a–c, Supplementary Movie 2).

Optovin is a rhodanine-containing small molecule with no previously annotated biological activity. Whereas DMSO-treated animals do not respond to photic stimuli, optovin-treated animals respond to light with vigorous motor excitation at an EC50 of 2 μM (Fig. 1d). Optovin-treated animals respond to 387 nm (violet) stimuli, but not to 485 nm (blue), 560 nm (green) or longer wavelengths (Supplementary Fig. 1a). Motor behavior in optovin-treated animals is elicited by stimulus intensities greater than 1.6 $\mu W*mm^{-2}$ (Fig. 1e). For stimuli lasting between 5 and 20 seconds, stimulus and response duration are proportional (Supplementary Fig. 2). In treated animals, multiple responses can be triggered with repeated light pulses (Fig. 1f). To determine the long-term effects of optovin exposure on development, behavior and survival, we analyzed the development, behavior and survival of zebrafish exposed to optovin (10 μM) for 96 hours. We did not identify any differences in the appearance, touch response, heart rate, fin movements, morphology or percentage survival between the treated and untreated groups (Supplementary Fig. 3). Thus, optovin is a novel behavior-modifying compound that causes rapid and reversible motor excitation in response to violet light stimuli.

To determine if optovin's mechanism of action could be predicted via behavioral profiling[27,29], we compared optovin's behavioral profile to the behavioral profiles of 700 annotated neuroactive compounds tested in triplicate. These compounds included ligands targeting the adrenergic, serotonergic, histaminergic, dopaminergic, cholinergic and glutamatergic pathways. Hierarchical clustering showed that the optovin phenotype is dissimilar to phenotypes caused by the annotated compounds, and clusters on a separate branch of the dendrogram (Supplementary Fig. 1b). These data suggest that optovin is functionally distinct from the known neuroactive compounds we tested. To gain insight into optovin's mechanism of action, we profiled optovin using the National Institutes of Mental Health Psychoactive Drug Screening Program (NIMH PDSP) to determine its activities against a panel of human and rodent CNS receptors, channels and transporters. No sub-micromolar targets were identified (Supplementary Table 1, Supplementary Fig. 4),

suggesting that optovin may act through a mechanism of action not represented in the extensive NIMH-PDSP collection.

Optovin structure activity relationship analysis

To determine the chemical features responsible for optovin's biological activity, we analyzed the structure activity relationships of various optovin analogs (Fig. 2). The optovin chemical structure contains three rings— a pyridine, a pyrrole, and a rhodanine ring (Fig. 2a). To determine if the pyridine ring is necessary for optovin activity, we tested two compounds in which this ring is replaced by either a benzene ring or a methyl group (6b8 and 6c1 respectively). Both compounds are bioactive, indicating that the pyridine ring is not required for optovin activity (Fig. 2a). To determine the importance of the pyrrole ring, we tested two compounds in which this ring is either removed entirely or replaced with a dimethylaniline ring (compounds 6c5 and 6c7 respectively). Neither analog retains activity, indicating that the pyrrole ring, or a close structural analog (as in compound 4g6), is necessary for the optovin response (Fig. 2a). Finally, to determine if the rhodanine ring is necessary, we analyzed the effects of four additional compounds. Two out of four rhodanine modifications abrogate the optovin response (compounds 6c2 and 6c3). By contrast, nitrogen methylation or replacing the rhodanine ring with hydantoin retains optovin activity (compound 6c4) (Fig. 2a). Interestingly, the duration of effect varies considerably among these different analogs, from 1.5s to 9s (Fig. 2b–c). Together, these observations suggest that optovin's biological activity depends on specific structural features that can be fine-tuned for shorter- or longer-lasting effects.

TRPA1 is necessary and sufficient for optovin activity

Optovin-treated zebrafish embryos respond to light at very early stages of development—before the eye and vision develops. This suggests that the optovin response is a non-visual behavior, and that optovin acts on tissues other than the eye. To determine if the eyes are necessary for the optovin response, we compared the responses of intact zebrafish embryos to the trunks of age-matched spinalized preparations transected posterior to the hindbrain. Sensory neurons in the trunk normally respond to various kinds of touch, stretch, temperature and pain, but not to light. Surprisingly, we found that optovin-treated spinalized preparations also responded to light (Supplementary Fig. 5, Supplementary Movie 3). Using a 405 nm laser beam, we observed optovin-dependent motor responses of the trunk, tail, and fins – all sites innervated by sensory neurons. Together, these data indicate that visual pathways are not necessary for the optovin-induced light response, and suggest that optovin may act on sensory neurons.

To determine if optovin acts on sensory neurons, we used calcium imaging to compare the activity of treated and untreated dorsal root ganglia (DRG) sensory neurons isolated from wild type mice. We found that optovin strongly activated 33% (35/105) of DRG neurons (Fig. 3a). This activation did not occur when optovin treatment occurred in the dark (Supplemantary Fig. 6 a–d). To determine if optovin activates neurons that also respond to known ligands, we treated the DRG neurons with mustard oil, a TRPA1 ligand[30]. We found that mustard oil activated 27% (28/105) of DRG neurons and that nearly all DRG sensory neurons that responded to mustard oil also responded to optovin (27/28) (Supplemantary

Fig. 6 b,d,e). These data suggest that optovin acts on a molecular target expressed in mustard oil responsive mammalian DRG sensory neurons; perhaps on TRPA1 itself.

TRPA1 channels play important roles in detecting chemical, thermal, and mechanical stimuli in a variety of organisms[31–33]. To test the hypothesis that optovin acts on TRPA1, we analyzed the behavior of TrpA1 mutant animals. The zebrafish genome encodes two orthologs of the mammalian TrpA1 gene, designated TrpA1a and TrpA1b, with different expression patterns and functions[34]. As expected, we found that wild-type zebrafish responded to optovin and the 387nm light stimulus with a prolonged motor excitation (Fig. 3b, c). TrpA1a homozygous mutants also responded to optovin (Supplementary Fig. 7). By contrast, TrpA1b homozygous mutant fish failed to respond (Fig. 3b, c). Importantly, dark-adapted TrpA1b mutant fish still exhibited normal control behaviors, like the PMR and the touch response, indicating that the TrpA1b mutation does not suppress motor behaviors in general (Supplementary Fig. 8). These data indicate that TrpA1b is necessary for the optovin response in zebrafish. To determine if the TrpA1 gene is also necessary for the optovin response mice, we analyzed the activity of DRG neurons isolated from TrpA1 mutant mice[11]. Unlike wild-type controls, TrpA1 mutant neurons did not respond to either mustard oil or optovin, although they did respond to KCl a depolarizing agent (Figure 3a). HC-030031, a selective TRPA1 antagonist[35], blocked optovin activity on these cells (Supplementary Fig. 6f). Together, these data suggest that TrpA1 is necessary for the optovin response.

To determine if TRPA1 is sufficient for optovin activity, we analyzed current density amplitudes via whole-cell patch clamping in HEK293T cells transfected with the human TrpA1 (hTrpA1) gene. We found that optovin activated cells transfected with hTrpA1 but not GFP, TRPV1 or TRPM8 (Fig. 3d, Supplementary Fig. 9). Similarly, we found that current density amplitudes in response to positive voltage steps were significantly increased in optovin-treated transfected cells following photo-stimulation, but not in cells lacking optovin, hTrpA1, or light (Supplementary Fig. 10). Together, these data suggest that the hTrpA1 gene is sufficient to confer optovin sensitivity to cultured HEK cells.

Optovin is a reversible photoactivated TRPA1 ligand

How might optovin activate TRPA1? When molecules absorb light, photons can excite electrons from their ground state to a triplet excited state via intersystem crossing[36]. These photoactivated compounds can then undergo reactions by transferring energy or electrons to target molecules, including aqueous molecular oxygen. Optovin is a yellow-colored compound with peak absorbance at 415 nm (Fig. 4a). To determine if optovin is photochemically reactive, we exposed it to increasing intensities of 415 nm light and assayed for reactive oxygen species (ROS) generation. We found that optovin generates singlet oxygen ($^1O_2$), but neither hydroxyl radicals nor superoxide (Fig. 4b and Supplementary Fig. 11). Together, these data suggest that light excites optovin to a photochemically reactive state that can activate TRPA1 either directly or via singlet oxygen. Neither catalase nor superoxide dismutase reduced optovin's effects on hTRPA1 transfected HEK cells (Supplementary Fig. 12), further suggesting that hydroxyl radicals and superoxide do not contribute to optovin's activity.

To determine if photochemical energy transfer is necessary for optovin's behavioral phenotype, we analyzed the behavior of animals co-treated with DABCO, a singlet oxygen quencher and triplet energy acceptor[37]. We found that DABCO completely suppressed the optovin response *in vivo*, but did not affect other light elicited behaviors, like the PMR (Fig. 4c, Supplementary Fig. 13). These data suggest that photochemical energy transfer is necessary for optovin's behavioral effects. Reactive electrophilic compounds activate TRPA1 channels through the covalent modification of specific cysteine residues including those at amino acid positions 621, 633, and 856. Point mutations in these cysteines can reduce hTRPA1 activation by specific ligands without disrupting overall channel function[38–40]. To determine if these cysteine residues are also important for TRPA1 activation by optovin, we measured intracellular calcium levels in cells transfected with wildtype and mutant hTRPA1 channels. We found that cells transfected with WT channels showed a strong activation in response to light and optovin. By contrast, cells transfected with the C621S, C633S, C633S/C856S, or the triple cysteine mutant (3CK) channel showed a significantly decreased response (Fig. 4d–e, Supplementary Fig. 14). Together, these data suggest that optovin activates TRPA1 channels via a photoactivated intermediate that reacts with key redox-sensitive cysteine residues in the channel.

Rhodanine and hydantoin are photoelectric moieties used in photovoltaic panels and other photochemical applications[41,42]. Nevertheless, photosensitization alone is likely insufficient to grant optovin its unusual biological activity. For example, optovin is phenotypically unique compared to 171 additional rhodanine-containing compounds contained in the screening library (Supplementary Fig. 15). In addition, we found that only optovin causes behavioral excitation, while other photosensitizers that also generate singlet oxygen do not (Fig. 4c). These data suggest that generation of singlet oxygen alone is insufficient for optovin's behavioral effects, and that structure-dependent interactions are important for optovin to activate TRPA1 *in vivo*.

One possible explanation for optovin's activity is that photo-excited optovin directly alkylates cysteine residues in TRPA1 via rapid and reversible covalent bonding. By analogy, previous work has shown that a reversible thioether bond forms between Cys325 of the ERRα receptor and the α,β-unsaturated alkene group of a rhodanine-like small molecule[43]. To determine if a similar reaction may occur between optovin and TRPA1, we measured the activity of a methylated optovin analog in which the methyl group is predicted to hinder thioether bond formation. We found that optovin and the unmethylated analog 7c7 both cause light-dependent motor excitation *in vivo* (Fig. 4 c,f). By contrast, the methylated analog 7d1 did not cause light dependent motor activity (Fig. 4c,f). These data suggest that thioether bond formation may be important for optovin to activate TRPA1, although we cannot exclude the possibility that methylation alters other properties of the molecule besides thioether bond formation.

Photochemical control of optovin-treated animals

Optovin's capacity to function in intact adult animals will impact its utility for future clinical and research applications. Thus, we analyzed the effects of 405 nm laser illumination on optovin-treated adult animals. In zebrafish, we found that illuminating the dorsal fin elicited

rapid and reversible contraction of the fin, but did not appear to otherwise disturb the treated animal (Supplementary Movie 4). To determine if fin contraction was voluntary or involuntary, we repeated the experiment using spinalized preparations. Optical control of dorsal fin contraction was preserved in spinalized animals treated with optovin (Fig. 5a). Furthermore, we found that carefully controlled laser illumination of specific regions along the body of spinalized zebrafish produced specific dorsal, ventral, and lateral tail movements reminiscent of those used by intact fish during swimming (Figure 5b, Supplementary Movie 5, 6). Because zebrafish TRPA1 is primarily expressed in sensory neurons, these contractions and swimming behaviors likely occur via activation of spinal reflex arcs. These data indicate that optovin enables real-time optical control of neurons in adult wild-type vertebrate animals. We found that optovin also elicited nociceptive behaviors in adult mice (Fig. 5c). Thus, optovin shows activity on adult animals *in vivo*, and may be preferable to conventional TRPA1 ligands for achieving high-resolution spatiotemporal control.

Discussion

These studies have identified optovin, a small molecule that enables optical control of endogenous channels and neuronal signaling in wild-type non-transgenic animals. Optovin differs from previously identified photochemical switch compounds in several significant ways. Optovin acts on TRPA1 channels, which were previously inaccessible via optical techniques. Unlike reversibly caged glutamate and photoswitchable affinity label compounds, optovin is not based on azobenzene photoreactivity. In addition, optovin can be washed out and appears to be quite selective in its activity, with no significant activity at dozens of other potential targets tested.

Optovin was discovered in a behavior-based chemical screen. As with most compounds discovered in phenotype-based screens, determining optovin's mechanism of action has been a central focus of our studies. Through genetic, molecular, and electrophysiological experiments, we have identified optovin's cellular target (sensory neurons) and have found that optovin acts on the cation channel TRPA1 in these cells. Several lines of evidence indicate that TRPA1 channels are both necessary and sufficient for optovin function. 1) Genetic mutation of TrpA1b in zebrafish completely eliminates optovin's activity. 2) In a heterogeneous population of mouse DRG neurons, all optovin-responsive neurons also respond to the TRPA1 agonist mustard oil. 3) Non-excitable cultured cells can be rendered light-sensitive by transfection with the hTrpA1 gene. Together, these data suggest that optovin specifically targets TRPA1 to enable the light-based control of sensory neurons.

Illumination of many small molecules, including optovin, can produce singlet oxygen or other reactive oxygen species. Nevertheless, it does not appear that TRPA1 is simply responding to optovin-generated singlet oxygen, because none of the efficient singlet oxygen-generating compounds that we tested caused any behavioral excitation in zebrafish. Instead, we favor the hypothesis that optovin binds directly to TRPA1 and forms a photo-dependent and reversible covalent adduct, perhaps through a radical coupling with a cysteine residue in TRPA1. Olefins like the one found in optovin's α,β-unsaturated rhodanine system are known to react with cysteines under physiological conditions[43,44]. In addition, alterations to optovin or TRPA1 that would prevent cysteine adduct formation reduce

optovin activity: methylation of optovin's olefin dramatically reduces its activity, as does mutation of presumptive target cysteines in TRPA1. These data are consistent with formation of a thioether linkage between TRPA1 and optovin (see model in Supplementary Figure 16).

Precedent exists for specific and reversible formation of cysteine adducts between small molecules and their targets. A series of electron-deficient olefins was recently shown to undergo rapid thiol addition reactions with a cysteine in their target kinase. The resultant thioether adducts are short lived, with the reverse reaction (thiol elimination) occurring spontaneously on sub-second to second timescales[44]. In another example that is perhaps even more analogous, flavin mononucleotide (FMN) is bound non-covalently by LOV domain-containing proteins[45]. Illumination with blue light excites FMN to the triplet state such that the C(4a) carbon of FMN reacts with a nearby cysteine in the LOV domain, forms a covalent adduct, and alters the protein structure and function. This thioether adduct is also spontaneously reversible on the timescale of seconds. In both of these examples, non-covalent interactions are necessary to bring the small molecule into close proximity to the target cysteine where a transient thioether linkage forms spontaneously (electron-deficient olefins) or upon photoactivation (FMN). That structure-directed induced-proximity may also be necessary in the case of optovin is supported by the fact that 171 similar rhodanines in our screening collection did not activate TRPA1 during the screen.

If optovin forms a thioether linkage with TRPA1, it appears to be photo-dependent and reversible. Its photo-dependence is suggested by the fact that even high concentrations of optovin do not elicit a behavioral response in zebrafish in the dark. Furthermore, when zebrafish or DRG neurons are treated with optovin and rinsed prior to illumination, no excitation is observed. Therefore, optovin does not appear to modify TRPA1 in the absence of light. After illumination, excitation is sustained for several seconds, and different optovin derivatives sustain excitation for differing lengths of time after illumination ends, from about 1 second (4g6) to more than 9 seconds (6b8). These observations are consistent with the idea that termination of excitation is mediated by reversal of the thioether adduct formation and that structural features of the optovin derivatives control the rate of reversal. More extensive analysis will be required to elucidate the factors that influence the reversal rate.

It will be interesting to learn if optovin-like molecules have utility for controlling endogenous receptors in organisms other than the zebrafish and mice. We have shown that optovin activates TRPA1 from zebrafish, mouse and humans, and that optovin elicits light-dependent behaviors in zebrafish and mice. Optovin's activity in gating human TRPA1 in transfected cells suggests that it could in theory be applied to humans, but development of these compounds for therapeutic applications will require further chemical optimization. For example, rhodanine-containing compounds have been characterized by some as too reactive for direct clinical development, and only one rhodanine-containing compound is in current clinical use[45]. Therefore, the safety of optovin-like compounds in humans will need to be evaluated. Nevertheless, the ability to control endogenous TRPA1 channels *in vivo* raises a number of therapeutic possibilities ranging from pain relief to spinal trauma therapy. Although optovin's activity appears largely restricted to TRPA1-expressing neurons,

additional screening may identify next generation compounds targeting a wide range of targets in different excitable cell types, including cardiac cells. Such tools would have applications ranging from basic neuroscience research to clinical interventions.

ONLINE METHODS

Aquaculture

A large number of fertilized eggs (up to 5,000 embryos per day) were collected from group mating of Ekkwill or TuAB zebrafish. Embryos were raised in HEPES (10 mM) buffered E3 media in a dark incubator at 28 °C until 30 hpf. Groups of ~8 embryos (28 hpf) were distributed into the wells of flat bottom black-walled 96 well plates filled with E3 media (360 μl). Embryos were then incubated in a dark incubator 25 °C for chemical treatment and subsequent experiments. All zebrafish protocols were approved by the Institutional Animal Care and Use Committee at Massachusetts General Hospital.

Chemical libraries and treatments

The Actiprobe library (TimTec) contains 10,000 compounds dissolved in DMSO at a stock concentration of 1mg/ml (~3mM). The library was screened at a 1:300 dilution in E3 buffer for a final concentration of ~ 10 μM. Negative controls were treated with an equal volume of DMSO. Stock solutions were added directly to zebrafish in the wells of a 96 well plate, mixed, and allowed to incubate for 2–10 hours in the dark prior to behavioral evaluation in the PMR assay. The library (10,000 compounds) was purchased from the Tim Tec corporation. The Neurotransmitter Library (700 compounds; cat# 2810) was purchased from Biomol International. Reordered hit compounds were dissolved in DMSO and added to wells as described above. Ordering information: optovin (ST52606; TimTec), analog 6b8 (5707191; Chembridge), 6c1 (6092141; Chembridge), 6c5 (118192; Sigma), 6c7 (6211600; Chembridge), 6c2 (6176046; Chembridge), 6c3 (6206065; Chembridge), 6c4 (7030539; Chembridge), 4g6 (ST025379; TimTec). Reordered compounds were used as received; MS/NMR data were not collected to confirm their identities.

PMR Behavioral assay

Animals were exposed to a two pulse stimulus train with a 10s inter-stimulus interval. Exposure to the first pulse was used to trigger the photomotor response, which has a refractory phase of approximately 10 minutes. Untreated animals do not respond to the second pulse of light, so motor activity after the second pulse was used to assay for optovin activity. In a typical assay, 1000 frames of digital video were recorded at 33fps using a camera (Hamamatsu ORCA—ER) mounted on a microscope (Nikon TE200) with a 1× objective. Instrument control and data measurement were performed using custom scripts for Metamorph Software (Molecular Devices). Each video was saved for review. Light stimuli were generated with a 300-watt xenon bulb housed in a Lambda LS illuminator (Sutter) and delivered to the well 10s and 20s after the start of each video. A cold mirror (reflectance between 300 nm and 700 nm) on the illuminator was used to block wavelengths outside of this range. Light intensity was measured using a PM100D power meter attached to a S120VC photodiode power sensor (Thorlabs). Where indicated, filters were used to restrict the excitation light to the indicated wavelengths.

Spinalized preparations

Adult zebrafish (0.5–1.5 years) were briefly anesthetized in ice water and quickly decapitated with a sharp razor blade. Spinalized preparations were incubated in optovin (50 μM) for 1–2 min prior to testing with laser light stimuli (405 nm, 400 μW mm^{-2}).

Behavioral analysis

To analyze digital video recordings, custom software scripts were used to automatically draw six evenly spaced line segments across each well such that each embryo is likely to be crossed by one of the lines. The software then tracks the average intensity of the pixels for each segment over time. As the embryos move, the light intensity at some of the pixels changes. The motion index was calculated by taking the total absolute difference in pixel intensity between frames. This motion index correlates with the overall amount of motion in the well, both in terms of contraction frequency and number of animals in motion. Behavioral features are quantified by `excitation scores' that are calculated by taking the 75^{th} percentile of the motion index for 3–5s following the light stimulus. The behavioral profiles were clustered using Euclidean distance and average linkage clustering. All computations and figures were carried out with the Matlab statistical programming environment.

Statistical analysis

We used one-way ANOVA and the Tukey HSD post hoc test to test for significant differences between groups, generate 95% confidence intervals and identify groups with significantly different means. For groups with significant differences, we used the two-tailed t-test to test the null hypothesis and calculate the *p* value. Statistical analyses were performed using the *anova1*, *multcompare* and *ttest2* functions provided by the MATLAB statistics toolbox.

Electrophysiology

HEK293 cells were plated upon poly-lysine coated cover slips and transiently transfected with human TRPA1. Voltage clamp recordings were made in the whole-cell configuration 48 hours after transfection using glass electrodes with 2–4MOhm resistance when filled with (in mM) 140 CsCl, 2 Mg2ATP3, 2 MgCl, 5 EGTA, and 10 HEPES (pH adjusted to 7.2 with CsOH) and while bathed at room temperature in extracellular solution containing (in mM) 150 NaCl, 5.4 KCl, 1.8 CaCl2, 1 MgCl, and 5mM HEPES (pH adjusted to 7.4 with NaOH). A voltage ramp protocol from −80mV to +80mV over 400ms was repeated every second during the following conditions: while the cell was dialyzed by the pipette, followed by at least 60 seconds of illumination with 405nm light, after which optovin (10 μM) containing extracellular solution was perfused into the bath, followed by 1 minute of illumination. Current elicited at holding potentials of ±70mV as well as the slope of the current-voltage relation while ramping from 0 to +70mV were used to characterize TRPA1 activation.

NIMH PDSP profiling

Activity determinations were generously provided by the National Institute of Mental Health's Psychoactive Drug Screening Program, Contract # HHSN-271-2008-00025-C

(NIMH PDSP). Complete assay details are found on-line at: http://pdsp.med.unc.edu/UNCCH%20Protocol%20Book.pdf

Calcium Imaging Methods

C57Bl/6 male mice (3–4 weeks old) were decapitated and DRG were dissected into 4°C Hank's Balanced Salt Solution (HBSS; Gibco), then neurons were dissociated using collagenase (1 mg/mL; Worthington) and dispase (5 mg/mL; Gibco) dissolved in HBSS. Neurons were plated in Neurobasal-A medium (Invitrogen), supplemented with B-27 Supplement (Gibco), L-glutamine (Gibco), and penicillin-streptomycin (Gibco). The neurons were plated onto coverslips coated with 0.1 mg/mL poly-D-lysine (Sigma) and 5 μg/mL laminin (Sigma). After 24 h, neurons were washed with assay buffer (HBSS, supplemented with 9 mM HEPES, 11 mM D-glucose, 0.1% fatty-acid free BSA, pH 7.3) and incubated for 1 h with 2 μM Fura2-AM (Invitrogen) with 0.2% pluronic (Invitrogen) in assay buffer in the dark at room temperature. The neurons were then washed with assay buffer and allowed to equilibrate at room temperature for 30 min prior to imaging. After a 120 s baseline perfusion of assay buffer containing 3.3% DMSO, 100 μM optovin dissolved in the DMSO-assay buffer solution, or the DMSO-assay buffer solution alone as a control, was perfused onto the neurons for a period of 1 min. Fura-2 is activated with UV-light, and the process of imaging Fura-2 was enough to activate the optovin. As a no-light control to ensure that the presence of optovin alone did not cause activation, imaging was stopped for the 1-minute period of optovin treatment, and resumed once the solution perfused back onto the neurons. Following this one-minute period, cells were perfused with DMSO-assay buffer to remove the agonist, which was followed by addition of 100 μM mustard oil (in DMSO-assay buffer) to determine the total number of TrpA1-expressing neurons present. Images were acquired on a Nikon Eclipse Ti microscope (Nikon, Melville, NY). Neurons were counted as activated if they showed a response during the 1-minute activation period. All procedures involving animals for calcium imaging were approved by the Institutional Animal Care and Use Committee at the University of North Carolina at Chapel Hill.

HEK293 cells were plated onto poly-lysine-coated glass bottom culture dishes (MatTek Corp), and grown in Dulbecco's Modified Eagle's Medium (DMEM, Sigma) supplemented with 10% fetal bovine serum and 100U/mL penicillin and 100 μg/ml streptomycin. After 24 hrs, cells were transfected, according to manufacturer's instructions, in Opti-MEM media, using 4 μl lipofectamine 2000 (Invitrogen), 0.5 μg EGFP in pcDNA, and 0.3 μg TrpA1 DNA per dish. Media was replaced after 2 hours, and cells were cultured for an additional 17 hours. As previously described for neurons, HEK cells were washed with assay buffer (HBSS Gibco 14025, supplemented with 9 mM HEPES, 11 mM D-glucose, 0.1% fatty-acid free BSA, pH 7.3) and incubated for 1 h with 2 μM Fura2-AM (Invitrogen) with 0.2% pluronic (Invitrogen) in assay buffer in the dark at room temperature. The cells were then washed with assay buffer and allowed to equilibrate at room temperature for 30 min prior to imaging. At the start of the imaging session for each dish, cells were replaced with DMSO-assay buffer. After 50 seconds of imaging, assay buffer was aspirated by hand, and replaced with 100 μM optovin dissolved in the DMSO-assay buffer solution. Each dish of HEK cells was imaged for a total of 3 minutes.

Cells were transfected with the hTRPA1[38], TRPA1 C621S[38], hTRPA1 C633S[39] and hTRPA1 C633S, C856S[39] plasmids as described.

Assay for singlet oxygen generation using singlet oxygen sensor green (SOSG)

UV-vis absorption spectra were recorded at 20 μM in methanol using an Evolution 300 UV-Vis Spectrophotometer (Thermo Fisher Scientific Inc., Waltham, MA). 96-well black-sided plates were used for fluorescent probe experiments. SOSG (Molecular Probes Invitrogen, Eugene, OR) as a 1mM stock solution in DMF was added to give final concentration of 5μM SOSG, to optovin and analogues dissolved as 5μM solutions in 200μL 50% H_2O/CH_3CN preloaded in 96-well plates. An Omnilux Clear-U LED light source (Photo Therapeutics Inc), Carlsbad, CA) that emits blue light 415-nm±15-nm as a homogeneous spot with an irradiance of 50 mW/cm^2 measured with a power meter (model DMM 199 with 201 standard head; Coherent, Santa Clara, CA) that covers an area of one half of a 96-well plate. Fluorescence spectrophotometry was carried out with SpectraMax M5 plate reader (Molecular Devices, Sunnyvale, CA) using excitation and emission at 504 and 525-nm. Fluorescence was read after each successive increment of blue light was delivered. As a positive control for a known photosensitizer that absorbs 415-nm light with a quantum yield of singlet oxygen of approximately 0.6 we used a conjugate between polyethylenimine and chlorin(e6) (PEI-ce6)[46].

Long-term toxicity testing

To determine the long-term effects of optovin exposure on development, behavior and survival, we analyzed the development, behavior and survival of larvae (n=150) and adult zebrafish (n=2) exposed to optovin (10 μM) for 96 hours. We did not identify any differences between the appearance, touch response, heart rate, fin movements, or morphology between the treated and untreated groups.

NIMH PDSP in vitro receptor profiling

Supplemental Table 1. *In vitro* receptor profiling was performed by the National Institute of Mental Health's Psychoactive Drug Screening Program, Contract # HHSN-271-2008-00025-C (NIMH PDSP). For primary screening, data represent mean % inhibition at the indicated receptor subtypes (N = 4 determinations). The default primary screening concentration is 10 μM. If >50% inhibition was obtained in the primary screen, Ki determinations were performed at concentrations ranging from 10 pM to 10 μM. For Ki determinations, data represent Ki (nM) values obtained from non-linear regression. Complete assay details are found on-line at: http://pdsp.med.unc.edu/UNC-CH%20Protocol%20Book.pdf.

Statistical analysis

We used one-way ANOVA and the Tukey HSD post hoc test to test for significant differences between groups, generate 95% confidence intervals and identify groups with significantly different means. For groups with significant differences, we used the two-tailed t-test to test the null hypothesis and calculate the *p* value. Statistical analyses were performed using the *anova1*, *multcompare* and *ttest2* functions provided by the MATLAB

statistics toolbox (Mathworks). All error bars represent standard deviations, unless otherwise noted.

Dissection and culture

Male adult C57Bl/6 mice were purchased from Jackson Laboratories and housed in the animal facilities of Children's Hospital Boston on a 12 hour alternating light-dark cycle. Animals for imaging were dissected after 7 weeks of age. TRPA1-KO mice were provided by Kelvin Kwan[11]. After CO_2 asphyxiation and cervical translocation, and following spinal laminectomy, the left and right dorsal root ganglia (DRG) from the whole spine were removed and placed in 4°C Hanks buffered saline solution without calcium and magnesium (HBSS, Life Technologies). After the DRG were collected and spun down for 3 minutes at 1000 rpm (150 g), they were placed in a collagenase/dispase solution (3 mg/mL dispase II and 1 mg/mL collagenase A, Roche Applied Science) and allowed to incubate at 37°C for 90 minutes. After incubation the cells were washed in Dulbecco's Modified Eagle's Medium (DMEM, Life Technologies), fortified with 4.5 g/L D-glucose, L-glutamine, 110 mg/L sodium pyruvate, 10% fetal bovine serum (Life Technologies), penicillin (500 U/mL, cellgro), and streptomycin (500 μg/mL, cellgro). DNAse (125 U/mL, Sigma) was then added and the solution was triturated using successively smaller caliber flame-polished pasteur pipettes. This solution was gently layered onto a bovine serum albumin gradient (10% albumin from bovine serum, Sigma in PBS, Life Technologies) and spun at 150 g for 12 minutes. After removal of the supernatant, the cells were washed again in DMEM, suspended in neurobasal medium (Life Technologies) supplemented with L-glutamine (20 mM, Life Technologies), B-27 supplement (Life Technologies), penicillin (500 U/mL, cellgro), and streptomycin (500 μg/mL, cellgro) and then plated onto laminin-treated (1 mg/mL, Sigma) 15 mm glass-bottom dishes (MatTek Corporation), and then placed in an incubator at 37°C (5% CO_2) overnight. All imaging was performed one day post-dissection and culture.

Calcium Imaging

DRG neurons were imaged on a Nikon Ti Eclipse inverted microscope. Fura-2, AM (Life Technologies) was loaded into the neurons for 30 minutes (room temperature, 4 μg/mL). After washing with standard extracellular solution (Boston BioProducts), the cells were imaged using a QImaging EXi Aqua cooled camera and data was collected and analyzed using NIS Elements software (AR 3.10). Neurons were selectively exposed to various solutions via a gravity-assisted perfusion system. Responses were included if they were 20% greater than baseline.

Mouse Behavior

Male adult C57Bl/6 mice were assessed for behavior after 7 weeks of age, were purchased from Jackson Laboratories and housed in the animal facilities of Children's Hospital Boston on a 12 hour alternating light-dark cycle, being provided food and water *ad libitum*. This behavioral protocol was approved by the Institutional Animal Care and Use Committee at Children's Hospital Boston. After habituation periods in a custom-built behavior chamber, mice were either treated with 20 μL of optovin solution (15 mM in DMSO, Sigma-Aldrich)

or vehicle control (DMSO) on the ear. Upon return to the behavior chamber, a laser (405 nm, class 3A, i.e. common laser-pointer) was trained on the treated ear. Time to activation of a characteristic head-twitch or head-shake response (HSR) was recorded for each animal over five separate trials (Corne et al., 1963). The response is a rapid, radial twitch of the head about the dorsal-ventral axis of the head. The time cutoff for laser stimulation was set at 60 seconds if no response was elicited (4 optovin vs. 4 control animals). One optovin-treated mouse was excluded from the mean analysis due to extreme non-responsiveness. Average time to response per animal was calculated by a blinded coder using VLC media playback at .25× speed who measured the actual time the laser was on the ear. Data was pooled between animals within groups. Error bars represent standard error.

Supplementary Material

Refer to Web version on PubMed Central for supplementary material.

ACKNOWLDEGEMENTS

We thank Kelvin Kwan, David Corey, Takashi Miyamoto, Ardem Patapoutian, Tomohiro Numata and Yasuo Mori for human TrpA1 constructs. Alex Schier, David Prober and Drew Robson generously provided TrpA1 mutant zebrafish. We thank Rachelle Gaudet, Ahmet Vakkasglu, Brian Shoichet, Tim Dunn, Misha Ahrens, Florian Engert, Ralph Mazitschek and members of our research groups for helpful advice. This work was supported by NIH grants K01MH091449 (DK), MH086867 and MH085205 (RTP), the Charles and Ann Sanders MGH Research Scholar award (RTP), and the Michael Hooker Chair and the NIMH Psychoactive Drug Screening Program (BLR). M.J.Z. was supported by grants from NINDS (R01NS060725, R01NS067688), J.C-B. was supported by an NRSA training grant from NINDS (F31NS068038) and DJM was supported by NIH grants HL109004 and DA026982.

REFERENCES

1. Alexander GM, et al. Remote Control of Neuronal Activity in Transgenic Mice Expressing Evolved G Protein-Coupled Receptors. Neuron. 2009; 63:27–39. doi:10.1016/j.neuron.2009.06.014. [PubMed: 19607790]
2. Armbruster BN, Li X, Pausch MH, Herlitze S, Roth BL. Evolving the lock to fit the key to create a family of G protein-coupled receptors potently activated by an inert ligand. Proc Natl Acad Sci USA. 2007; 104:5163–5168. doi:10.1073/pnas.0700293104. [PubMed: 17360345]
3. Banghart M, Borges K, Isacoff E, Trauner D, Kramer R. Light-activated ion channels for remote control of neuronal firing. Nat Neurosci. 2004; 7:1381–1386. doi:10.1038/nn1356. [PubMed: 15558062]
4. Boyden E, Zhang F, Bamberg E, Nagel G, Deisseroth K. Millisecond-timescale, genetically targeted optical control of neural activity. Nat Neurosci. 2005; 8:1263–1268. doi:10.1038/nn1525. [PubMed: 16116447]
5. Deisseroth K. Optogenetics. Nat Meth. 2011; 8:26–29. doi:10.1038/nmeth.f.324.
6. Ferguson SM, et al. Transient neuronal inhibition reveals opposing roles of indirect and direct pathways in sensitization. Nat Neurosci. 2011; 14:22–24. doi:10.1038/nn.2703. [PubMed: 21131952]
7. Szobota S, et al. Remote control of neuronal activity with a light-gated glutamate receptor. Neuron. 2007; 54:535–545. doi:10.1016/j.neuron.2007.05.010. [PubMed: 17521567]
8. Janovjak H, Szobota S, Wyart C, Trauner D, Isacoff E. A light-gated, potassium-selective glutamate receptor for the optical inhibition of neuronal firing. Nat Neurosci. 2010; 13:1027–1032. doi: 10.1038/nn.2589. [PubMed: 20581843]
9. Volgraf M, et al. Reversibly caged glutamate: a photochromic agonist of ionotropic glutamate receptors. Journal of the American Chemical Society. 2007; 129:260–261. doi:10.1021/ja067269o. [PubMed: 17212390]

10. Wang S, et al. All optical interface for parallel, remote, and spatiotemporal control of neuronal activity. Nano letters. 2007; 7:3859–3863. doi:10.1021/nl072783t. [PubMed: 18034506]
11. Kwan KY, et al. TRPA1 contributes to cold, mechanical, and chemical nociception but is not essential for hair-cell transduction. Neuron. 2006; 50:277–289. doi:10.1016/j.neuron.2006.03.042. [PubMed: 16630838]
12. Kramer RH, Fortin DL, Trauner D. New photochemical tools for controlling neuronal activity. Curr Opin Neurobiol. 2009; 19:544–552. doi:10.1016/j.conb.2009.09.004. [PubMed: 19828309]
13. Callaway EM, Katz LC. Photostimulation using caged glutamate reveals functional circuitry in living brain slices. Proceedings of the National Academy of Sciences of the United States of America. 1993; 90:7661–7665. [PubMed: 7689225]
14. Dalva MB, Katz LC. Rearrangements of synaptic connections in visual cortex revealed by laser photostimulation. Science. 1994; 265:255–258. [PubMed: 7912852]
15. Fortin DL, et al. Photochemical control of endogenous ion channels and cellular excitability. Nature Methods. 2008; 5:331–338. doi:10.1038/nmeth.1187. [PubMed: 18311146]
16. Fortin DL, et al. Optogenetic photochemical control of designer K+ channels in mammalian neurons. Journal of neurophysiology. 2011; 106:488–496. doi:10.1152/jn.00251.2011. [PubMed: 21525363]
17. Noguchi J, et al. In vivo two-photon uncaging of glutamate revealing the structure-function relationships of dendritic spines in the neocortex of adult mice. The Journal of Physiology. 2011; 589:2447–2457. doi:10.1113/jphysiol.2011.207100. [PubMed: 21486811]
18. Volgraf M, et al. Allosteric control of an ionotropic glutamate receptor with an optical switch. Nature chemical biology. 2006; 2:47–52. doi:10.1038/nchembio756. [PubMed: 16408092]
19. Wieboldt R, et al. Photolabile precursors of glutamate: synthesis, photochemical properties, and activation of glutamate receptors on a microsecond time scale. Proc Natl Acad Sci USA. 1994; 91:8752–8756. [PubMed: 8090718]
20. Mourot A, et al. Rapid optical control of nociception with an ion-channel photoswitch. Nature Methods. 2012:1–9. doi:10.1038/nmeth.1897. [PubMed: 22312634]
21. Brain SD. TRPV1 and TRPA1 channels in inflammatory pain: elucidating mechanisms. Annals of the New York Academy of Sciences. 2011; 1245:36–37. doi:10.1111/j.1749-6632.2011.06326.x. [PubMed: 22211974]
22. Jordt SE, Ehrlich BE. TRP channels in disease. Sub-cellular biochemistry. 2007; 45:253–271. [PubMed: 18193640]
23. Kremeyer B, et al. A gain-of-function mutation in TRPA1 causes familial episodic pain syndrome. Neuron. 2010; 66:671–680. doi:10.1016/j.neuron.2010.04.030. [PubMed: 20547126]
24. Schwartz ES, et al. Synergistic role of TRPV1 and TRPA1 in pancreatic pain and inflammation. Gastroenterology. 2011; 140:1283–1291. e1281–1282. doi:10.1053/j.gastro.2010.12.033. [PubMed: 21185837]
25. MacRae CA, Peterson RT. Zebrafish-based small molecule discovery. Chem Biol. 2003; 10:901–908. [PubMed: 14583256]
26. Zon LI, Peterson RT. In vivo drug discovery in the zebrafish. Nature reviews Drug discovery. 2005; 4:35–44. doi:10.1038/nrd1606. [PubMed: 15688071]
27. Kokel D, et al. Rapid behavior-based identification of neuroactive small molecules in the zebrafish. Nature chemical biology. 2010 doi:10.1038/nchembio.307.
28. Schmitt EA, Dowling JE. Early retinal development in the zebrafish, Danio rerio: light and electron microscopic analyses. J Comp Neurol. 1999; 404:515–536. [PubMed: 9987995]
29. Rihel J, et al. Zebrafish behavioral profiling links drugs to biological targets and rest/wake regulation. Science. 2010; 327:348–351. doi:10.1126/science.1183090. [PubMed: 20075256]
30. Dhaka A, Viswanath V, Patapoutian A. TRP ION CHANNELS AND TEMPERATURE SENSATION. Annual review of neuroscience. 2006; 29:135–161. doi:10.1146/annurev.neuro.29.051605.112958.
31. Bandell M, et al. Noxious cold ion channel TRPA1 is activated by pungent compounds and bradykinin. Neuron. 2004; 41:849–857. [PubMed: 15046718]

32. Moran MM, Xu H, Clapham DE. TRP ion channels in the nervous system. Curr Opin Neurobiol. 2004; 14:362–369. doi:10.1016/j.conb.2004.05.003. [PubMed: 15194117]
33. Escalera J, von Hehn CA, Bessac BF, Sivula M, Jordt SE. TRPA1 mediates the noxious effects of natural sesquiterpene deterrents. The Journal of biological chemistry. 2008; 283:24136–24144. doi:10.1074/jbc.M710280200. [PubMed: 18550530]
34. Prober D, et al. Zebrafish TRPA1 Channels Are Required for Chemosensation But Not for Thermosensation or Mechanosensory Hair Cell Function. Journal of Neuroscience. 2008; 28:10102–10110. doi:10.1523/JNEUROSCI.2740-08.2008. [PubMed: 18829968]
35. Eid SR, et al. HC-030031, a TRPA1 selective antagonist, attenuates inflammatory- and neuropathy-induced mechanical hypersensitivity. Molecular pain. 2008; 4:48. doi: 10.1186/1744-8069-4-48. [PubMed: 18954467]
36. Laustriat G. Molecular mechanisms of photosensitization. Biochimie. 1986; 68:771–778. [PubMed: 3019431]
37. Ouannes. Quenching of singlet oxygen by tertiary aliphatic amines. Effect of DABCO (1, 4-diazabicyclo [2.2. 2] octane). 1968
38. Macpherson LJ, et al. Noxious compounds activate TRPA1 ion channels through covalent modification of cysteines. Nature. 2007; 445:541–545. doi:10.1038/nature05544. [PubMed: 17237762]
39. Takahashi N, et al. TRPA1 underlies a sensing mechanism for O2. Nature chemical biology. 2011; 7:701–711. doi:10.1038/nchembio.640. [PubMed: 21873995]
40. Hinman A, Chuang HH, Bautista DM, Julius D. TRP channel activation by reversible covalent modification. Proceedings of the National Academy of Sciences of the United States of America. 2006; 103:19564–19568. doi:10.1073/pnas.0609598103. [PubMed: 17164327]
41. Barton HJ, Bojarski JT. Photoinduced stereospecific formation of substituted hydantoin from hexobarbital. Journal of Photochemistry and Photobiology A. 1990
42. Marinado T, Hagberg DP, Hedlund M. Rhodanine dyes for dye-sensitized solar cells: spectroscopy, energy levels and photovoltaic performance. Physical Chemistry. 2009
43. Patch RJ, et al. Identification of diaryl ether-based ligands for estrogen-related receptor alpha as potential antidiabetic agents. Journal of medicinal chemistry. 2011; 54:788–808. doi:10.1021/jm101063h. [PubMed: 21218783]
44. Serafimova IM, et al. Reversible targeting of noncatalytic cysteines with chemically tuned electrophiles. Nature chemical biology. 2012; 8:471–476. doi:10.1038/nchembio.925. [PubMed: 22466421]
45. Herrou J, Crosson S. Function, structure and mechanism of bacterial photosensory LOV proteins. Nature reviews. Microbiology. 2011; 9:713–723. doi:10.1038/nrmicro2622. [PubMed: 21822294]
46. Tegos GP, et al. Protease-stable polycationic photosensitizer conjugates between polyethyleneimine and chlorin(e6) for broad-spectrum antimicrobial photoinactivation. Antimicrobial agents and chemotherapy. 2006; 50:1402–1410. doi:10.1128/AAC.50.4.1402-1410.2006. [PubMed: 16569858]
47. Corne SJ, Pickering RW, Warner BT. A method for assessing the effects of drugs on the central actions of 5-hydroxytryptamine. British journal of pharmacology and chemotherapy. 1963; 20:106–120. [PubMed: 14023050]

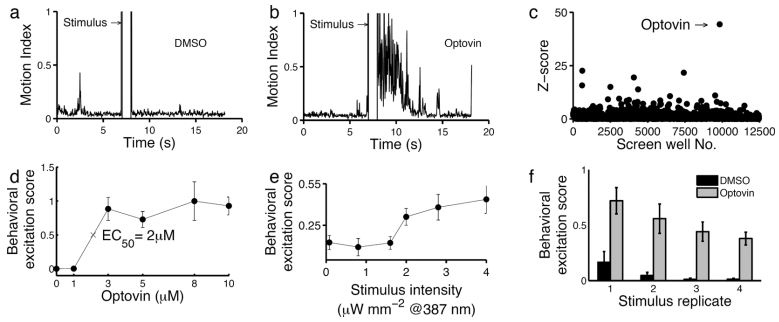

Figure 1. Identification of optovin, a compound enabling light-mediated neuronal excitation

Plots showing the zebrafish behavioral response of DMSO (a) and optovin (b) treated animals. The bar indicates the timing of a 1s white light stimulus. (c) Scatter plot showing the behavioral excitation scores from chemical the screen (12,500 individual wells). The *y*-axis represents the number of standard deviations of each excitation score from the control mean (Z-score). The labeled arrow indicates the well treated with optovin. (d) Dose response curve showing optovin's effects on animal behavior (EC_{50}=2 μM; n= 5). The difference between the 1 μM and 3 μM treatments is significant, $p<0.001$. (e) Line plot showing excitation scores at the indicated stimulus intensities (n=5). The difference between groups treated at 1.6 μW*mm^{-} and 2 μW*mm^{-2} is significant, $p<0.001$. (f) Bar plot showing behavioral responses to repeated light stimuli (n=5). Differences between treated and untreated groups are significant, $p<0.001$.

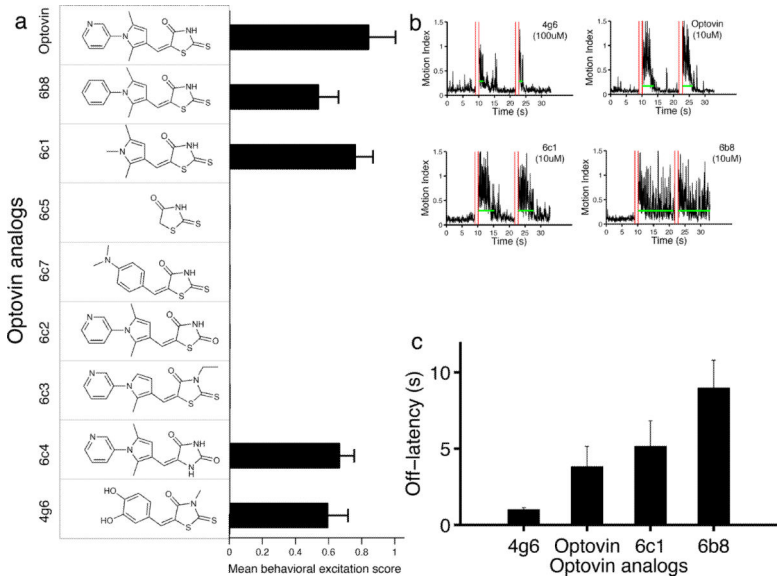

Figure 2. Optovin structure activity relationship analysis

(a) Horizontal bar plot showing behavioral excitation scores from groups treated with the indicated optovin analogs (n=5). Optovin, 6b8, 6c1, 6c4 and 4g6 analogs are active; 6c5, 6c7,6c2, and 6c3 are inactive. Differences between active and inactive groups are significant, $p<0.001$. Structures of the analogs are shown to the left of the bar plot. All compounds were tested at 10 μM, except for the 4g6 analog, which was tested at 100 μM. (b) Example responses from the indicated groups. Red vertical lines indicate light stimuli. Green horizontal lines indicate the off-latency duration for motor responses following each stimulus. (c) Bar plot showing average behavioral response duration of groups treated with the indicated optovin analogs. Values are means ± standard deviations (n=5). Differences between optovin and 4g6 and 6b8 are significant, $p<0.01$.

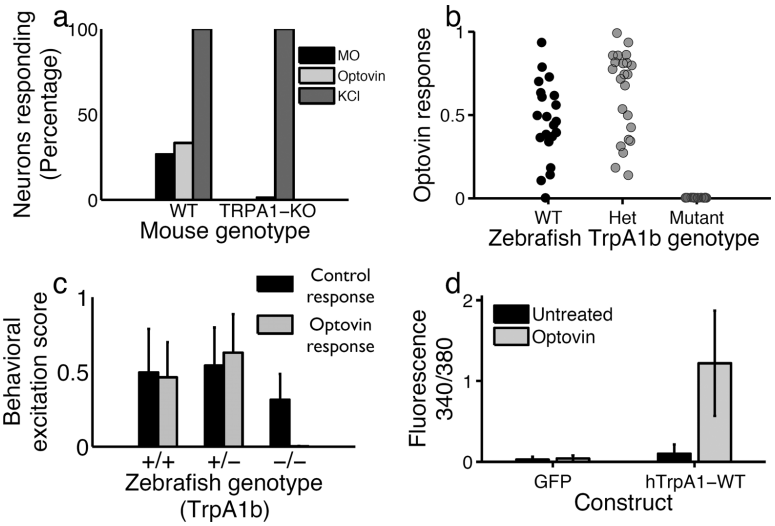

Figure 3. TRPA1 is necessary and sufficient for the optovin response

(a) Percentage of mouse DRG neurons responding to the indicated treatments. In wild type, the light stimulus activated 30% of neurons assayed (35/105). In the TRPA1-KO neurons, the total percentage of responding neurons was 2.7% (8/291). (b) Behavioral excitation scores during the optovin response for zebrafish of the indicated genotypes. (c) Behavioral excitation scores calculated for WT, heterozygous and homozygous TrpA1b mutant animals (n=21, 23 and 16 respectively) during the PMR (control) and optovin response assays. Homozygous mutant animals show a significantly lower activity during the optovin response assay, $p<0.001$. (d) Bar plot showing calcium indicator dye fluorescence in cells transfected with GFP or hTrpA1 before and after a 2 min treatment with optovin and light (n=130, 120 cells). The difference between treated and untreated hTRPA1 transfected cells is significant, $p<0.001$.

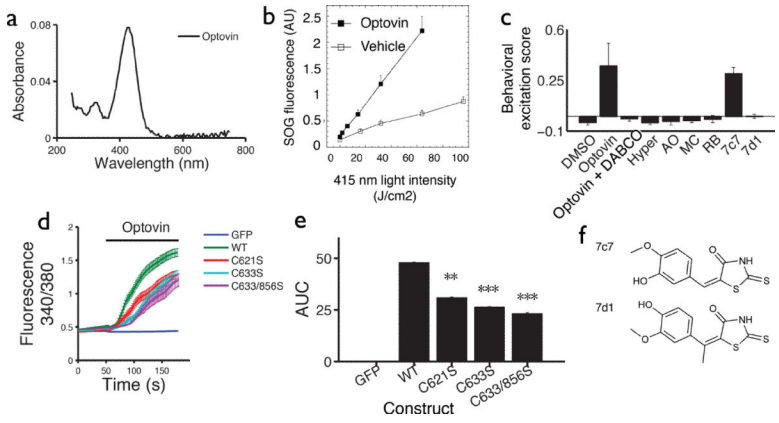

Figure 4. Optovin activates TRPA1 via structure dependent photochemical reactions

(a) Optovin's absorbance (UV-Vis) at the indicated wavelengths. (b) Fluorescence of the singlet oxygen indicator dye SOG with and without optovin at the indicated light intensities. (c) Behavioral excitation scores from animals treated with the indicated compounds (n=5 wells). Wells treated with optovin and 7c7 are significantly higher than DMSO treated controls, $p<0.001$). The difference between DMSO and 7d1 is not significant, $p=0.8$. Abbreviated names of singlet oxygen generators: Hyper, Hypericin; AO, acridine orange; MC, merocyanine 540; RB, rose Bengal. (d) Calcium indicator fluorescence before and after optovin treatment in cells transfected with the GFP, hTRPA1 or the indicated hTRPA1 mutant construct. (e) Barplot quantifying the calcium response 1 min after optovin treatment (n=130, 120, 107, 111, 75 cells respectively) (**$p<0.01$, ***$p<0.0001$). (f) Structures of the analogs are shown. Note that the olefin is methylated in analog 7d1. All compounds were tested at 10 μM.

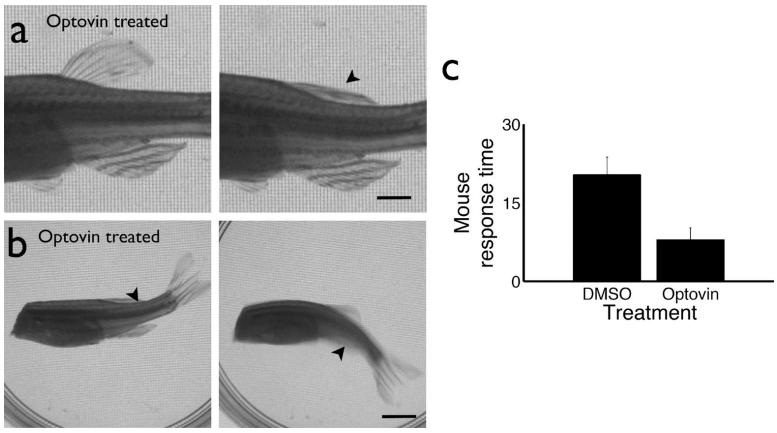

Figure 5. Remote control of optovin treated animals

(a) Photographs of spinalized zebrafish before and after photo-stimulation of the dorsal fin. Scale bar, 2.5 mm. (b) Photographs of spinalized zebrafish responding to laser photo-stimulation. Arrowheads indicate approximate location of the 405 nm laser point stimulus. Scale bar, 5 mm. (c) Male C57Bl/6 mice were given an optovin (15 mM) or vehicle (DMSO) swab on one ear. A low-power laser (405 nm) was trained on that ear, while time to a characteristic head shake or head twitch was measured. The difference between groups is significant ($p < 0.05$). Values are averages ± SEM.